34th Annual International Conference of the IEEE EMBS
San Diego, California USA, 28 August - 1 September, 2012

Fabrication and successful in-vivo implantation of a flexible neural implant with a hybrid polyimide-silicon design

Alexandru Andrei[1], Nina Tutunjyan[2], Greet Verbinnen[3], Steven VanPut[4], Olga Krylychkina[1]
Wolfgang Eberle[1], Silke Musa[1]

***Abstract*— A flexible neural implant was designed and fabricated using an novel integration approach that offers the advantages of both silicon and polymer based implants: high density electrodes and precise insertion on one side and mechanical flexibility suitable for reduced tissue strain due to micro-motion during chronic implantation on the other side. This was achieved by separating the device into silicon or polymer areas, depending on their desired functionality. The tip, where the recording and stimulation electrodes would be placed, was kept of silicon: a choice that doesn't call for any compromise to be made regarding the high density electrode and possible local circuit integration later on. The bevel shaped sharp silicon tip also proved to facilitate the probe insertion, offering a behavior very much similar to the classical rigid silicon probes. On the other side, most of the 1 cm long shank of the probe was made out of polyimide. This led to more than one order of magnitude reduction of the forces necessary to bend the shank. The flexible shank proved also to be more robust than silicon probes, sustaining significant deformation in any direction without fracture. The 9mm deep in-vivo implantation were successfully achieved without buckling for 10 μm/s and 100 μm/s insertion speeds.**

I. INTRODUCTION

The sustained tissue response during chronic implantation of neural implants is one of the main factors preventing long term neural activity recordings. The tissue strain around the implant has been identified to play an important role in this response [1]. The tissue deformation that occurs during the insertion can be reduced by optimizing the probe geometry and insertion speed [2]. However, it has been shown that the implant geometry has little influence on the chronic tissue response [3], this response being rather influenced by the probe - tissue often significant stiffness mismatch. Since in most cases the implant is fixed to the skull, the natural movement of the brain inside the skull due to brain pulsations (cardiac pulse and breathing) as well as micro-motion (rotational acceleration of the animal head) induces relative movements between the probe and the tissue. A finite element modeling study showed that the induced tissue strain could be significantly reduced if the silicon would be replaced by softer polymer materials [4]. Implant solutions using polymers have been successfully demonstrated [5], [6], [7]. However, the increased shank flexibility often makes these devices difficult to insert without buckling. Structural stiffening has been suggested as a potential solution, such as the inclusion of metal [8] or silicon [9] inserts.

The objective of the present work was to fabricate a neural implant with improved long-term recording capabilities trough a hybrid design that offered both the mechanical flexibility of polymer based probes and the precise stereotactic insertion without buckling together with the high density electrode and possible local circuit integration offered by classical silicon micro-machined silicon implants.

II. MATERIALS AND METHODS

A. Design and process flow

The implant consisted of three distinct parts as shown in Fig. 1: a rigid bevel shaped 220 μm wide silicon tip for the stimulation and recording electrodes, a 9 mm long polyimide shank providing the desired probe flexibility and a rigid silicon body. The probe had a constant thickness of 65 μm along its three distinct parts. 35 μm thick silicon inserts were used to mechanically reinforce the flexible polymer shank in the areas where a transition between flexible and rigid materials occurred.

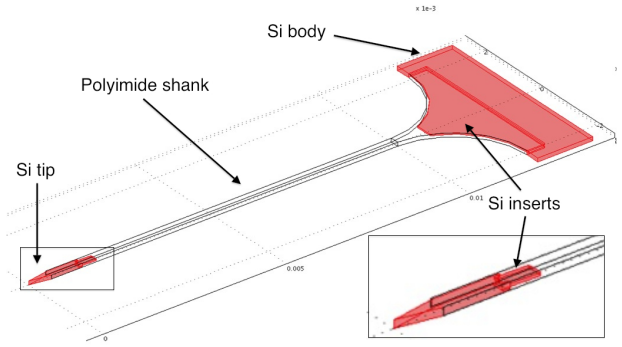

Fig. 1. 3D model of the neural implant. The silicon tip and body of the probe are highlighted while the polyimide shank is transparent.The distance between the tip and the place where the shank becomes wider is 1 cm.

The process flow summarized in Fig. 2 shows how the device was fabricated through a succession of front side deep silicon etch of a staircase structure filled with polymer material, followed by front and back side planarization and thinning steps. The staircase structure required for the definition of the silicon inserts was realized using a SiO_2 hard mask pattern defined in the 1^{st} step and a photoresist mask

[1]A. Andrei, O. Krylychkina, W. Eberle and S. Musa are with the Bio-Electronic Systems Group, Imec, 75 Kapeldreef, 3001 Leuven, Belgium andreial@imec.be, krylych@imec.be, eberle@imec.be, musa@imec.be
[2]N. Tutunjyan is with the Dry Etch Group, Imec, 75 Kapeldreef, 3001 Leuven, Belgium tutun@imec.be
[3]G. Verbinnen is with the CMP and Thinning Group, Imec, 75 Kapeldreef, 3001 Leuven, Belgium gverbin@imec.be
[4]S. VanPut is with the Information Technology Department, CMST, 914 Technologiepark, 9052 Gent, Belgium svanput@intec.ugent.be

defined in the 2^{nd} step. During this 2^{nd} step, an initial deep silicon etch was performed with a target depth of 40 μm. After the resist was stripped, in step 3, a second deep silicon etch was performed in order to etch 30 μm of the previously resist protected areas. Consequently, the areas that have been already etched in step 2, were further etched down to a final depth of 70 μm. The deep silicon etch was performed in an Adixen DSiE ICP system (Alcatel) using a pulsed etching technique of subsequent etch and passivation steps, currently known as a Bosch type process.

The deep silicon trenches were filled by four successive spin coat operations of PI2611 polyimide (HD Microsystems), in step 4. This particular polymer was chosen for its low moisture uptake, low stress and 8.5 MPa Young modulus, which is about three times higher than most other polyimides. Its low residual stress ensured a final device with a straight shank as shown in Fig. 3, while its increased stiffness was important for precise insertion without buckling.

The polymer covering the tip and body silicon areas was planarized in step 5, using a Disco tool in two stages: an initial rough grinding that removed most of the excess polymer, followed by a fine grinding step that reduced the final surface roughness. The planarization left about 5 μm of polyimide covering the tip and body areas of the implant that were removed by an oxygen based dry etch process developed in a 2300 Exelan CCP chamber (Lam Research).

The wafer was thinned by temporally bonding its front side to a carrier and grinding its backside down to a final thickness of 65μm. At this point, all the silicon material connecting the tip and body parts of the probes was removed, with the polyimide filling the front side trenches becoming exposed (step 6). The devices were however still connected across the wafer by the polyimide filling the trenches defining the probe outline. This undesired polymer material was removed in step 7 by laser ablation performed in a custom tool equipped with a 20 μm spot size YAG laser.

By dissolving the temporal bonding glue with a solvent, the devices detached from the carrier wafer and were placed on a dedicated printed circuit board package, as it is schematically shown in the last step of Fig. 2. Fig. 3 shows a picture of such a packaged device. This prototype is a mechanical dummy manufactured for our flexibility and insertion feasibility experiments but had no electrical recording capabilities. Electrical functionality could be added to such a device by patterning the electrodes and metal lines in additional process steps.

B. Mechanical testing

The flexibility of the polyimide shank was tested in an Xyztec Condor 250 system by recording the force during the displacement of the probe tip 3 mm in the vertical direction (perpendicular to the top surface of the device) and 1.3 mm in the horizontal direction (perpendicular to the side walls of the shank). The displacements were limited to these values in order to avoid the slipping of the sensor tip along the probe shank during the vertical test as well as the twisting of the shank during the horizontal test. For comparison purposes,

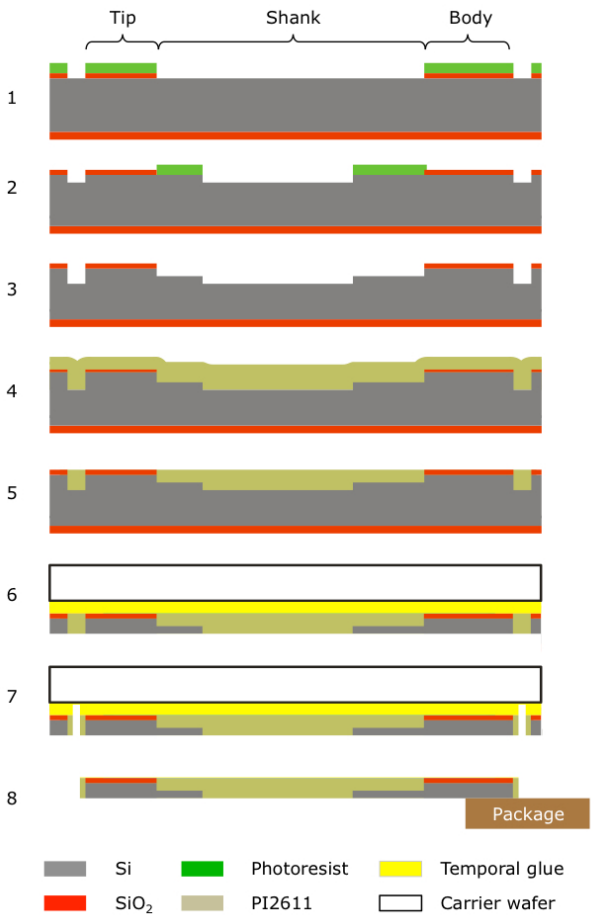

Fig. 2. Schematic cross section view of the main fabrication steps.

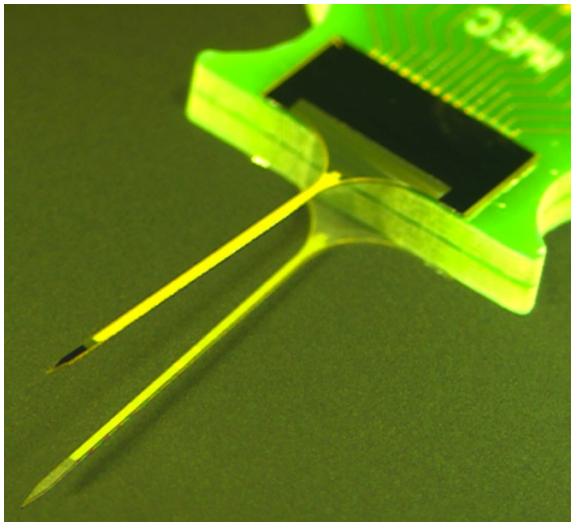

Fig. 3. Picture of a flexible probe that was used for the mechanical tests and in-vivo insertion experiments.

the same tests were performed with silicon neural implants without a polymer shank but with the same geometry and dimensions.

C. In-vivo implantation experiment

Two flexible neural implants were inserted in the right and left hemispheres of a wistar rat with the head positioned in a stereotactic frame and placed under general anesthesia by chloral hydrate and local anesthesia by Xylocaine. The dura was carefully cut and retracted making sure that the center of the exposed pia surface remained clean and undamaged. The probes were implanted with 10 μm/s and 100 μm/s insertion speeds using a electronically controlled hydraulic micro-drive. The insertion forces were recorded with a miniature load cell. A detailed description of this set-up has been published in several recent publications [2], [10], [11].

III. RESULTS AND DISCUSSION

A. Silicon inserts fabrication

Fig. 4 shows a scanning electron microscope image of the 40 μm high insert near the tip of the probe that is 70 μm high. The difference between the silicon areas exposed during the first and the second deep silicon etch steps required fine tuning of the process parameters and the extension of the standard 10% plasma on duty cycle time up to 20% for the first etch step and up to 30% for the second step [12]. Fig. 5 shows a detail of the resulting step structure having perfectly vertical and undamaged sidewalls.

B. Polyimide process

The fine grinding at the end of the planarization step was performed with a reduced spindle speed and dedicated grinding wheel that allowed a significant reduction of the average roughness of the polyimide surface down to 103 nm. The dry etch that removed the remaining 5 μm of polymer covering the tip and body areas was optimized in order to automatically stop when the silicon oxide surface became exposed. This was achieved by recording with optical emission spectrometry the concentration of the CO species in the chamber. The dry etch treatment further reduced the average polymer surface roughness down to 80 nm, and proved even more effective when a thin photo resist layer was deposited on the grinded polyimide before the dry etch treatment [12]. Fig. 6 shows an overview the wafer surface and buried silicon inserts after dry etch.

We found that the best compromise between cutting depth, local polymer melting and residue generation during the laser ablation of the polyimide was a power level of 50 mW with a scanning speed of 3mm/s (20 μm spot size). Four subsequent passes that removed each time about 20μm of material were necessary for the successful singulation of the devices.

C. Polyimide shank flexibility

When the tip of the implant was displaced vertically or horizontally, the force value increased linearly with the displacement. Table I shows the significant differences observed between the hybrid probe behavior and the silicon probe

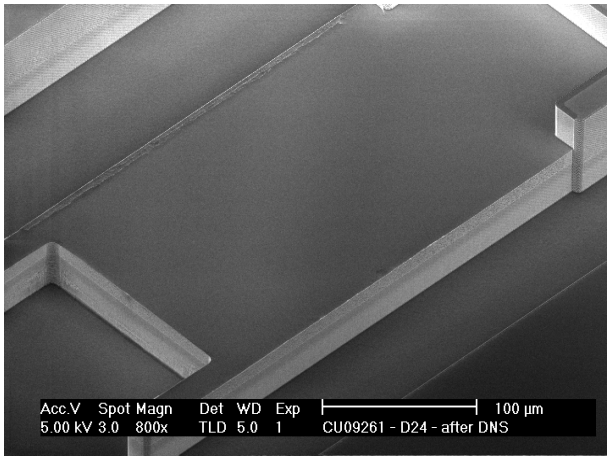

Fig. 4. Image of the insert shape on the tip side of the probe fabricated by the two step deep silicon etch technique developped in this study

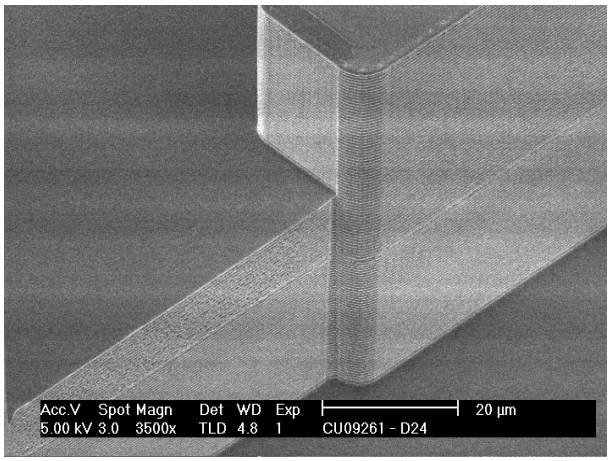

Fig. 5. Detail of the two step deep silicon etch sidewall profile.

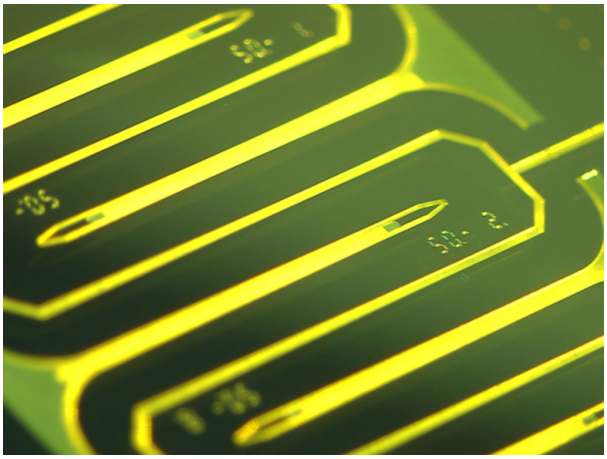

Fig. 6. Overview of the wafer after the dry etch front surface treatment leading to a top surface without any polyner

with similar dimensions. The later proved to be 26 times stiffer when solicited vertically. As expected, both probes were stiffer when solicited on the horizontal direction since the implant design was 220 μm wide for a thickness of only 65 μm. However, the flexible probe proved to be more robust, sustaining a tip displacement of 3 mm. Its silicon counter part broke when its tip was displaced only half this length. The maximum force value recorded at that moment was about 16 times higher than the one recorded for the flexible probe for equivalent displacement.

TABLE I

PROBE SHANK BENDING TEST RESULTS

Shank bending forces (mN)	Hybrid design	Silicon only
Vertical (3 mm)	0.48	13.3
Horizontal (655 μm)	2.51	40
Horizontal (1.3 mm)	5	-

D. In-vivo implantation

The in-vivo implantations were necessary to verify that even if the hybrid probes developed in this study proved to be significantly more flexible than silicon probes with identical geometry, they were also stiff enough for precise stereotactic insertion without buckling. The force required for the buckling of such a polymer probe has been approximately estimated analytically [13] to about 3 mN. This value was significantly higher than the forces required for the penetration of the pia of a silicon probe with similar geometry, estimated to be inferior to 1 mN for either 10 μm/s or 100 μm/s insertion speeds [2], [10]. Fig. 7 shows that the behavior of the hybrid flexible probes was found to be very similar to the insertion of their silicon equivalents: less than 1 mN penetration force and a dimpling inferior to 1 mm followed by a steady increase of the force during its full length insertion into the brain. As expected [2], the faster insertion speed lead to higher end of insertion force values, but no buckling was observed during the experiments.

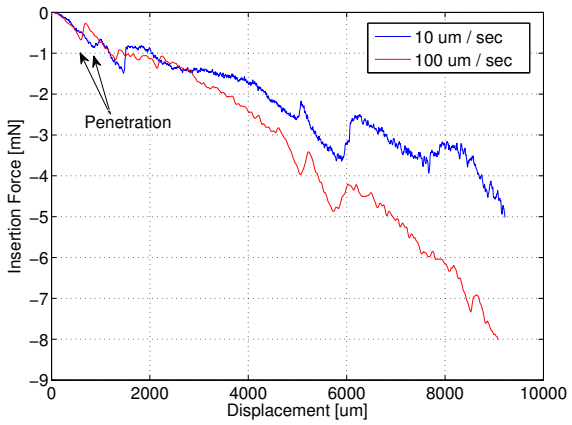

Fig. 7. Insertion force profile evolution with insertion depth for two different insertion speeds.

IV. CONCLUSION

The polyimde-silicon neural implant presented in this study proved to be significantly more flexible than silicon probes with same dimensions. Its reduced stiffness did not however impede on the precise stereotactic insertion trough pia mater of the probe. The in-vivo implantation was successfully achieved without any shank buckling. The insertion probe profile was found to be similar to the one observed for rigid silicon probes, since in our design the tip of the probe is still made of silicon. This novel integration approach that kept the recording and stimulation tip area of the implant made of silicon offers other significant advantages such as the possibility of integration of locally amplified high density electrode arrays in the tip, something difficult to achieve for other polymer based implant designs.

REFERENCES

[1] D. J. Edell, V. V. Toi, V. M. McNeil, and L. D. Clark, "Factors influencing the biocompatibility of insertable silicon microshafts in cerebral cortex," *IEEE Transactions on Biomedical Engineering*, vol. 39, pp. 635–643, 1992.

[2] A. Andrei, M. Welkenhuysen, B. Nuttin, and W. Eberle, "A response surface model predicting the in vivo insertion behavior of micromachined neural implants," *Journal of Neural Engineering*, vol. 9, p. 016005, 2012.

[3] D. Szarowski, M. D. Andersen, S. Retterer, A. Spence, M. Isaacsonc, H. Craighead, J. Turner, and W. Shain, "Brain responses to micromachined silicon devices," *Brain Research*, vol. 983, pp. 23–35, 2003.

[4] J. Subbaroyan, D. C. Martin, and D. R. Kipke, "A finite element model of the mechanical effects of implantable microelectrodes in the cerebral cortex," *Journal of Neural Engineering*, vol. 2, pp. 103–113, 2005.

[5] J. P. Seymour and D. R. Kipke, "Neural probe design for reduced tissue encapsulation in cns," *Biomaterials*, vol. 28, pp. 3594 – 3607, 2007.

[6] A. Mercanzini, K. Cheung, D. L. Buhl, M. Boers, A. Maillard, P. Colin, J.-C. Bensadoun, A. Bertsch, and P. Renaud, "Demonstration of cortical recording using novel flexible polymer neural probes," *Sensors and Actuators A*, vol. 143, pp. 90–96, 2008.

[7] C.-H. Chen, S.-C. Chuang, H.-C. Su, W.-L. Hsu, T.-R. Yew, Y.-C. Chang, S.-R. Yeh, and D.-J. Yao, "A three-dimensional flexible microprobe array for neural recording assembled through electrostatic actuation," *Lab On Chip*, vol. 11, p. 1647, 2011.

[8] A. A. Fomani and R. R. Mansour, "Fabrication and characterization of the flexible neural microprobes with improved structural design," *Sensors and Actuators A*, vol. 168, pp. 233–241, 2011.

[9] K. Lee, A. Singh, J. He, S. Massia, B. Kim, and G. Raupp, "Polyimide based neural implants with stiffness improvement," *Sensors and Actuators B*, vol. 102, pp. 67–72, 2004.

[10] A. Andrei, M. Welkenhuysen, L. Ameye, B. Nuttin, and W. Eberle, "Chronic behavior evaluation of a micro-machined neural implant with optimized design based on an experimentally derived model," in *Engineering in Medicine and Biology Society Conference (EMBC)*, IEEE, Ed., 2011.

[11] M. Welkenhuysen, A. Andrei, L. Ameye, W. Eberle, and B. Nuttin, "Effect of insertion speed on tissue response and insertion mechanics of a chronically implanted silicon-based neural probe," *IEEE Transactions on Biomedical Engineering*, vol. 58, no. 11, pp. 3250 – 3259, 2011.

[12] N. Tutunjyan, A. Andrei, G. Verbinnen, J. Slabbekoorn, and W. Eberle, "Dry etch challenges for implantable silicon-based. semi-flexible neural probe fabrication," in *Plasma Etch and Strip in Microelectronics*, 2011.

[13] K. Najafi and J. F. Hetke, "Strength characterization of silicon microprobes in neurophysiological tissues," *IEEE Transactions on Biomedical Engineering*, vol. 37, pp. 474–481, 1990.